

# High-Performance Materials for 3D Printing in Chemical Synthesis Applications

Frederik Kotz, Patrick Risch, Dorothea Helmer, and Bastian E. Rapp\*

3D printing has emerged as an enabling technology for miniaturization. High-precision printing techniques such as stereolithography are capable of printing microreactors and lab-on-a-chip devices for efficient parallelization of biological and biochemical reactions under reduced uptake of reactants. In the world of chemistry, however, up until now, miniaturization has played a minor role. The chemical and thermal stability of regular 3D printing resins is insufficient for sustaining the harsh conditions of chemical reactions. Novel material formulations that produce highly stable 3D-printed chips are highly sought for bringing chemistry up-to-date on the development of miniaturization. In this work, a brief review of recent developments in highly stable materials for 3D printing is given. This work focuses on three highly stable 3D-printable material systems: transparent silicate glasses, ceramics, and fluorinated polymers. It is further demonstrated that 3D printing is also a versatile technique for surface structuring of polymers to enhance their wetting performance. Such micro/nanostructuring is key to selectively wetting surface patterns that are versatile for chemical arrays and droplet synthesis.

## 1. Introduction

Miniaturization, that is, the transformation of scientific synthesis or analysis from standard labware dimensions (centi- to milliliters) to microscopic dimensions (micro- to nanoliters) holds several promises, for example, reduction of reactant uptake, reduction of processing time, and possibly massive parallelization.<sup>[1]</sup> The field of microfluidics deals with such small-scale processes, and many intricate lab-on-a-chip devices have been fabricated to facilitate complex analytical protocols in biology and biochemistry.<sup>[1]</sup>

Dr. F. Kotz, P. Risch, Dr. D. Helmer, Prof. B. E. Rapp  
Institute of Microstructure Technology (IMT)  
Karlsruhe Institute of Technology (KIT)  
Hermann-von-Helmholtz-Platz 1  
76344 Eggenstein-Leopoldshafen, Germany  
E-mail: Bastian.Rapp@kit.edu

 The ORCID identification number(s) for the author(s) of this article can be found under <https://doi.org/10.1002/adma.201805982>.

© 2019 The Authors. Published by WILEY-VCH Verlag GmbH & Co. KGaA, Weinheim. This is an open access article under the terms of the Creative Commons Attribution-NonCommercial-NoDerivs License, which permits use and distribution in any medium, provided the original work is properly cited, the use is non-commercial and no modifications or adaptations are made.

DOI: 10.1002/adma.201805982

Traditionally, microfluidic devices were fabricated via silicon or glass micromachining.<sup>[2,3]</sup> Silicon is structured by applying a mask and a subsequent wet or dry etching process. However, true 3D structures cannot be generated in silicon and optical analysis is not possible due to the intransparency of the material. Glasses, on the other hand, ensure high optical transparency, but glass micromachining usually also involves the generation of masks and consecutive etching with hazardous chemicals like hydrofluoric acid or using lasers for direct structuring.<sup>[4]</sup> The complicated nature of these structuring processes paved the way for polymers in microfluidics, which are much easier to process and to structure.<sup>[5]</sup> The triumphant success of polydimethylsiloxane (PDMS) is mainly attributed to its convenient processability and the high optical transparency, which made micro-

fluidic devices accessible to any standard laboratory, without having access to specialized equipment.<sup>[6]</sup> For the aqueous environment of biochemical assays, PDMS devices are therefore still the preferred choice for many researchers. However, the chemical resistance of these materials for the use in chemical synthesis is limited. In addition, classical soft replication of PDMS or subtractive machining approaches to structure polymeric chips are not capable of producing 3D chip designs and always require polymer bonding technologies since the production of suspended channels inside the bulk materials is not possible. Additive manufacturing, the layer-by-layer generation of a component, holds the great promise of reducing the polymer structuring process to a single step of fabrication using one machine and only requiring a digital model of the desired structure.<sup>[7]</sup>

3D printing has already had a huge impact on the field of microfluidics, because it enables the fabrication of complex integrated chips designs and prototypes in a minimal amount of time in the early phase of product development.<sup>[7,8]</sup> Different printing technologies have been demonstrated to being capable of fabricating microfluidic reactors, for example, fused deposition modeling (FDM), inkjet printing, and stereolithography (SL).<sup>[9–11]</sup> Stereolithography (a printing technique that cures photocurable resins layer-by-layer using light) remains the technology of choice for the fabrication of microfluidic reactors because it combines high resolution with affordable equipment and supply prices.<sup>[12]</sup> However, most of the applications

of lab-on-a-chip devices focus on detection and analysis of biomolecules in aqueous conditions. With environmental concerns and health issues mounting, the next logical step is miniaturization of chemical reactions. This would greatly facilitate the combinatorial synthesis of chemical libraries and has the potential to revolutionize, for example, drug discovery which still relies on screening large numbers of chemically synthesized substances to discover new active species. Although microreactor technology is a field which has seen significant scientific interest over the years, application demonstration has mostly been limited by the lack of suitable materials for chemical applications.<sup>[13,14]</sup> Traditionally, microreactors are commonly made from metals which limits their usability for chemical synthesis applications as they do not withstand corrosive conditions (i.e., strong bases and/or acids), are non-transparent and can only be machined to simple geometries as required, for example, in heat exchangers.<sup>[15,16]</sup> Recently, many attempts have been made to bridge the gap between microfluidics and chemistry. Flow-through “chemistry-on-chip” synthesis has the potential to revolutionize chemistry by ensuring more stable reaction conditions and new reaction pathways: ultrafast mixing, kinetic reaction control, or thermodynamic nonequilibrium conditions which are inaccessible via standard batch synthesis.<sup>[17–19]</sup> Heterogeneous reactions can run more efficiently in microfluidic format due to the large surface-to-volume ratios that ensure improved phase contact and heating is much easier controllable on the microscale which significantly enhances the yield of temperature-sensitive reactions.<sup>[20]</sup> Flow synthesis is therefore a powerful tool for improving reactions that are very sensitive to specific reaction parameters that significantly increase the yield in reactions with very expensive reactants and in general for the automation of synthesis in parallel.<sup>[21]</sup>

3D printing technologies have also been used for the fabrication of low-volume chemical batch or flow-through synthesis reactors.<sup>[21–23]</sup> These reactors have, for example, been used for the synthesis of small pharmaceutical molecules.<sup>[24]</sup> However, as mentioned above high-resolution manufacturing of microfluidic flow-through reactors requires SL printing. This is a major problem when merging these two fields since traditional polymer formulations used for SL are largely incompatible with the harsh conditions of chemical reactions.<sup>[22,25]</sup> Most regular materials for SL are acrylic- or epoxy-based possessing low chemical and thermal stability, 3D-printed polytetrafluoroethylene (PTFE), and polyimides being a notable exception.<sup>[26,27]</sup> Additionally, it has been shown that the polymeric materials often strongly influence the success of the reaction.<sup>[24]</sup> Thus, there is a need for novel highly resistant materials for SL.

Additionally, fine-tuning of materials and material formulations for 3D printing also opens up the potential to control the inherent micro-/nanostructuring of the bulk material. Combined with high lateral resolution, such structuring may be used to create polymeric materials with significantly enhanced properties compared to the nonstructured version. We have recently shown the fabrication of such a material system with the introduction of *Fluoropor*, an optically transparent fluoropolymer foam that can be structured using 3D printing techniques for generating surfaces with enhanced wetting properties, such as hydrophobic/superhydrophobic patterns.<sup>[28]</sup> Much

effort is made to produce such selectively wetted surfaces also for organic compounds to facilitate synthesis in droplets and the fabrication of chemical arrays.

The key to developing novel materials for precision SL lies in carefully combining polymerization initiators, inhibitors, and monomeric species to give liquids of adequate viscosity to enable high-resolution printing of microstructures or microvoids. Ideally, materials for chemical synthesis should possess high chemical and thermal stability as well as a high optical transparency for online analysis. In this article, we highlight recent developments in the field of novel materials for precision 3D printing with a focus on chemically resistant and stable materials. We will focus on high-precision 3D printing of fused silica glass, one of the most chemically and thermally stable materials, ceramics, and the most inert type of polymers, fluoropolymers.

## 2. Transparent Glass

Transparent silicate glasses are one of the most important materials in chemistry due to their high chemical and thermal stability combined with their outstanding optical transparency. Glasses are therefore widely used, for example, for classical glassware and batch reactors as well as for chemically resistant microfluidic chips.<sup>[13]</sup> However, it took more than two decades for the first 3D-printed transparent silicate glasses to emerge. Many attempts like selective laser sintering or melting or inkjet printing of glass powders had been proposed but led to white, porous, and nontransparent glass components.<sup>[29,30]</sup> The first successful approach to 3D-printed transparent glass was described by the group of Neri Oxman who used a modified fused deposition modeling approach whereby a low melting soda lime glass was heated to a temperature of  $\approx 1040$  °C and the melt was deposited through a nozzle.<sup>[31]</sup> An alternative approach used manually fed glass fibers which were molten using a laser beam.<sup>[32]</sup> However, both processes result in glass parts with very coarse structures which cannot be used to 3D print chemical reactors or high-resolution microfluidic chips for flow-through synthesis (see **Table 1**). In addition, both are direct glass printing processes and perform the printing process at elevated temperatures requiring special expensive printing equipment. Besides direct printing of glass, indirect printing processes have evolved. The first indirect printing process was developed by our group using silica nanocomposites that can be cured by light and turned into transparent high-quality fused silica glass via thermal debinding and sintering.<sup>[33]</sup> The nanocomposites consist of amorphous silica nanoparticles dispersed in a photocurable binder matrix.<sup>[34,35]</sup> We have shown that these nanocomposites can be printed using benchtop stereolithography in a layer-by-layer based fashion and turned into fused silica glass during a final heat treatment (see **Figure 1a**). Using microstereolithography and lithography, fused silica glass can be structured at resolutions of a few micrometers and a surface roughness of a few nanometers (see **Figure 1b**). The physical and chemical material properties of the resulting sintered fused silica glass are indistinguishable from commercial fused silica glass. They show the same high optical transparency in the UV, visible, and infrared region, the same mechanical strength,

**Table 1.** Comparison of relevant methods for high-resolution 3D printing of glass.

Method	Resolution	Solid loading [vol%]	Linear shrinkage	Processing time post treatment	Literature
Direct glass 3D printing					
Fused deposition modeling	>1 mm	–	–	–	[77]
Laser melting of glass fibers	>1 mm	–	–	–	[32]
Indirect glass 3D printing					
Stereolithography nanocomposites	60 $\mu\text{m}$	40–60 vol%	Isotropic 16–26%	$\approx$ 46 h	[33,35]
Stereolithography sol-gel precursor	$\approx$ 600 $\mu\text{m}$	n.a.	Non-isotropic XY $\approx$ 40–56% Z $\approx$ 33–48%	>7 d	[37]
Direct ink writing colloidal sol	$\approx$ 200 $\mu\text{m}$	10–20 vol%	Isotropic 41–53 vol%	112 h	[36]

and the same thermal and chemical resistance like commercial fused silica glass.<sup>[33]</sup> Alternative direct glass printing processes such as direct ink writing of colloidal silica suspensions and SL printing of photocurable sol-gel precursors (mixture of a photocurable silane and tetraethylorthosilicate) have also been described (see Figure 1c,d).<sup>[36–38]</sup> Both processes allow printing fused silica glass with resolutions of a few hundred micrometers. Direct ink writing has even been shown for multiple glass types ( $\text{SiO}_2/\text{SiO}_2\text{-TiO}_2$ ) in a single print.<sup>[39]</sup> A major challenge when printing nanocomposites, colloidal suspensions, or sol-gel-precursors is the linear shrinkage during drying and the postprocessing time during the final heat treatment. The shrinkage during the heat treatment depends on the solid loading of the printed resins. A high solid loading results in a low shrinkage of the part and reduces the risk of part damage during drying and the subsequent sintering process. This is a

major drawback of direct ink writing of silica suspensions and direct printing of sol-gel precursors which have solid loadings between 10 and 20 vol% resulting in a high linear shrinkage of up to 50%. In addition, Cooperstein et al. reported that printing sol-gel solutions using stereolithography results in a nonisotropic linear shrinkage which further complicates component design (see Table 1). High shrinkage and low solid loadings are major hurdles when working with sol-gel precursors or colloidal suspensions making the fabrication of macroscopic parts very time consuming.<sup>[40,41]</sup> The drying process of the printed sol-gel precursors and colloidal suspensions takes up to several days even for simple geometries (see Table 1).<sup>[36,37]</sup> Nanocomposites, on the other hand, have been demonstrated to have solid loadings of up to 60 vol% resulting in a linear shrinkage of only 15.66 vol%. Even parts with centimeter thickness could be thermally debound and sintered in  $\approx$ 46 h.

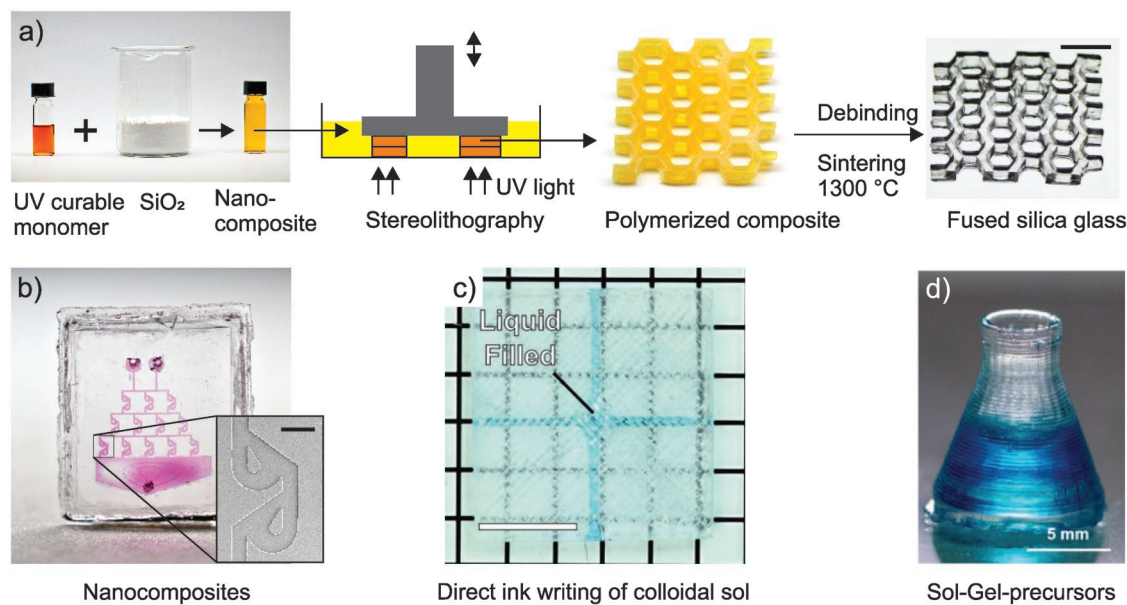


**Figure 1.** 3D printing of transparent glass. a) Stereolithography printing of silica nanocomposites. Amorphous silica nanoparticles are dispersed in an acrylic photocurable binder matrix. The nanocomposites can be printed using stereolithography printers. The printed part is then converted to a transparent fused silica glass via thermal debinding and sintering (scale bar: 7 mm). b) Microfluidic Tesla mixer fabricated using microlithography (scale bar: 200  $\mu\text{m}$ ). (a,b) Reproduced with permission.<sup>[33]</sup> Copyright 2017, Springer. c) Cavity filled with dyed water printed using direct ink writing of colloidal silica suspensions (scale bar: 4 mm). Reproduced with permission.<sup>[36]</sup> Copyright 2017, Wiley. d) Erlenmeyer flask printed using hybrid sol-gel precursors in a stereolithography printer. Reproduced with permission.<sup>[37]</sup> Copyright 2018, American Chemical Society.

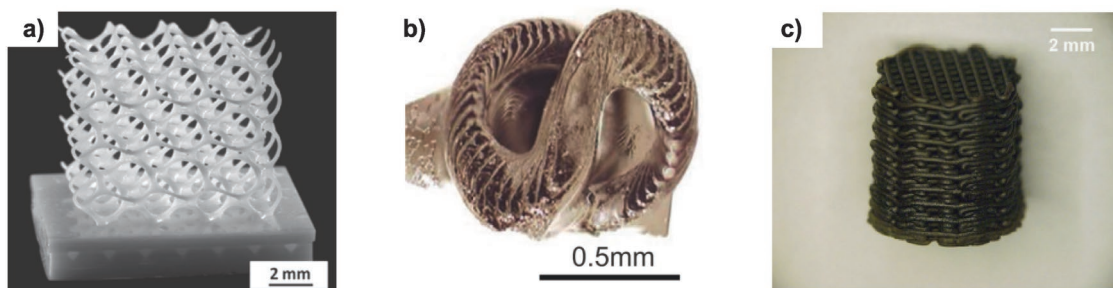


**Figure 2.** 3D printing of ceramics: a) Cellular tube fabricated by stereolithography printing of alumina nanocomposites and subsequent thermal debinding and sintering. Reproduced with permission.<sup>[45]</sup> Copyright 2014, John Wiley and Sons. b) Cork screw printed using preceramic polymers. Reproduced with permission.<sup>[47]</sup> Copyright 2017, Science. c) Robocasted heterogeneous ceramic catalyst fabricated by printing an  $\text{Al}_2\text{O}_3/\text{Cu}$  slurry and subsequent sintering at  $1400\text{ }^\circ\text{C}$ . Reproduced with permission.<sup>[52]</sup> Copyright 2016, Elsevier.

### 3. Ceramics

Ceramics are an interesting class of materials in chemical synthesis due to their high thermal and chemical resistance and the possibility to integrate catalytic active components into the ceramic.<sup>[42]</sup> 3D printing of ceramics using high-resolution SL consists of two main strategies: printing of photocurable composites or using preceramic polymers.<sup>[43]</sup> Photocurable composites consist of ceramic particles (ideally nanoparticles) in a photocurable binder matrix. Similar to fused silica glass printing described above, these composites can be printed using SL and then turned into a dense ceramic using thermal debinding and sintering. Some thermally and chemically resistant ceramics like alumina have been printed with high resolution using stereolithography (see **Figure 2a**).<sup>[44,45]</sup> Pre-ceramic polymers were first introduced in the 1960s. Upon heat treatment they can be pyrolyzed from organosilicon polymers into different relevant ceramics for chemical synthesis like SiC or SiOC.<sup>[46]</sup> Recently, preceramic polymers also entered the field of high-resolution stereolithography printing. Eckel et al. and Zanchetta et al. demonstrated nearly simultaneously that SiOC ceramics can be 3D printed using stereolithography printing with a resolution of a few hundred micrometers using functionalized preceramic polymers (see **Figure 2b**).<sup>[47,48]</sup> Higher resolutions of a few hundred nanometers have been demonstrated for SiCN ceramics using two-photon polymerization.<sup>[49]</sup> However, so far neither ceramic composites nor preceramic polymers have been used for direct 3D printing of high-resolution ceramic flow-through reactors. Since composites usually possess high viscosities, direct printing of microfluidic reactors is challenging since the removal of uncured material out of microchannels becomes more difficult with increasing viscosity.<sup>[50]</sup> Here, preceramic polymers with adjustable rheological properties could in future work become an interesting alternative for direct patterning of high-resolution components for chemical synthesis applications.

Ceramics have recently been more widely used for 3D printing of structured heterogeneous ceramic catalyst.<sup>[51]</sup> Tubío et al. printed a reusable copper catalyst system using robocasting of a  $\text{Cu}/\text{Al}_2\text{O}_3$  slurry.<sup>[52]</sup> The printed woodpile structures (see **Figure 2c**) were subsequently dried and sintered at  $1400\text{ }^\circ\text{C}$ . The performance of the printed  $\text{Cu}/\text{Al}_2\text{O}_3$  structures was demonstrated in different Ullmann reactions for the

synthesis of imidazoles, benzimidazoles, and N-aryl amides. Robocasting has been further used to print zeolite ZSM-5 in a water-based binder containing silica and bentonite. The printed catalysts were subsequently used for separation experiments of  $\text{CO}_2/\text{N}_2$  and  $\text{CO}_2/\text{CH}_4$  mixtures.<sup>[53]</sup>

### 4. Fluorinated Polymers

While glasses are the preferred materials for chemistry due to their high chemical and thermal stability, polymers are sometimes chosen as they do not require specialized equipment for printing and/or thermal post processing such as sintering.<sup>[5]</sup> However, most polymers used in 3D printing possess low chemical stability, especially when being exposed to organic solvents. Fluoropolymers are an exception, because fluorination leads to very low surface energies, that is, fewer liquids are capable of wetting fluorinated surfaces. The difluoromethylene ( $-\text{CF}_2-$ ) group, difluoromethyl group ( $-\text{CF}_2\text{H}$ ), and trifluoromethyl group ( $-\text{CF}_3$ ) possess surface energies of only  $\approx 18$ ,  $\approx 15$ , and  $\approx 6\text{ mN m}^{-1}$ , respectively. For comparison, methyl groups ( $-\text{CH}_3$ ) possess surface energies of  $\approx 23\text{ mN m}^{-1}$ .<sup>[54]</sup> Additionally, the carbon/fluorine bond is the shortest bond in organic chemistry making fluorinated polymers highly stable when exposed to a wide variety of reagents and solvents. One of the most well-known and important fluorinated polymers is PTFE also known under the trademark *Teflon* (by Dupont) originally discovered by Roy J. Plunkett. PTFE combines excellent chemical inertness, high thermal stability (up to  $260\text{ }^\circ\text{C}$ ), low friction coefficient, and low surface energies. However, 3D printing of PTFE is challenging due to its insolubility, high melting point, and high melt viscosity.<sup>[55,27]</sup> In 2016, 3M commercialized a process for 3D printing PTFE.<sup>[56]</sup> In this approach, PTFE nanoparticles are dispersed in a photocurable binder matrix and this nanocomposite is then printed using stereolithography. After the printing process, the binder is removed in a subsequent debinding step and the particles are sintered at around  $370\text{--}400\text{ }^\circ\text{C}$ . Zhang et al. demonstrated that similar nanocomposites can be printed using microstereolithography with tens of micrometer resolution (**Figure 3a**).<sup>[27]</sup> Until now these materials have not been used for 3D printing of chemical synthesis reactors. However, as PTFE is opaque the resulting PTFE reactors are intransparent and thus do not

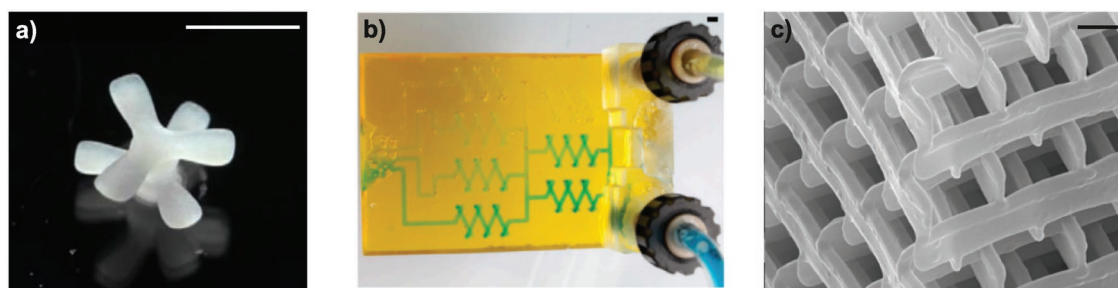


**Figure 3.** 3D printing fluorinated polymers: a) *Teflon* part printed using stereolithography and sintering (scale bar: 1 mm). Reproduced with permission.<sup>[27]</sup> Copyright 2018, IEEE. b) Microfluidic mixer structure fabricated by using PFPE methacrylates and commercial stereolithography printers (scale bar: 2 mm). Reproduced with permission.<sup>[64]</sup> Copyright 2017, MDPI. c) High-resolution woodpile structure in PFPE-based resin structured using two-photon polymerization (scale bar: 2  $\mu$ m). Reproduced with permission.<sup>[65]</sup> 2013, American Chemical Society.

allow online analysis during a chemical synthesis in a microfluidic chips.

Perfluoropolyether (PFPE) polymers are an interesting alternative for the fabrication of chemically resistant devices. Besides being chemically very stable, they exhibit high optical transparency to visible light, low surface energy, and tunable elasticity making them interesting candidates for chemically resistant microfluidic valves.<sup>[57,58]</sup> PFPE acrylates were first introduced by Priola et al. and were intensively used for the fabrication of chemically resistant microfluidic chips using PFPE acrylates as a casting material or a negative photoresist.<sup>[59–62]</sup> However, due to their high chemical resistance the bonding of these replicated or directly structured chips remains a major problem.<sup>[63]</sup> Here, 3D printing can make a huge difference since closed channel structures can be directly printed. We have recently shown that PFPE acrylate resin formulations can be printed using commercially available stereolithography printers.<sup>[64]</sup> Figure 3b shows an exemplary microfluidic gradient generator with a channel height and width of 800  $\mu$ m. The printed PFPE acrylates show high chemical stability when exposed to organic solvents. Higher resolutions can be fabricated by structuring hybrid triacrylate/PFPE-dimethacrylate resin formulations using two-photon lithography (2PL).<sup>[65]</sup> Figure 3c shows the scanning electron microscope image of a 50  $\mu$ m  $\times$  50  $\mu$ m  $\times$  50  $\mu$ m woodpile structure printed using 2PL. However, due to the serial nature of 2PL, these components can usually only be fabricated with small footprints which is usually insufficient for microfluidic synthesis applications. However, the combination of printing mesoscale channel structures using stereolithography and small functional microcomponents like membranes or filters using 2PL could open up new manufacturing approaches in the future to fabricate more complex microfluidic reactors in highly resistant PFPE-acrylates.

## 5. Fluorinated Polymers with Enhanced Performance

By introducing further carefully chosen additives into the liquid formulations for 3D printing, the performance of the resulting material can be fine-tuned due to adaptations in the inherent bulk material structure. These changes in morphology are self-organized and therefore do not require intricate control of the manufacturing process. Introducing a nano/microstructure

can significantly modulate the wetting properties of surfaces, because the structure can reduce the contact area between droplet and surface similar to the well-known lotus effect of the lotus leaf where a deposited water droplet only touches the pinacles of the structured surface of the leaf. We have recently shown that superhydrophobic fluorinated polymer foams can be fabricated by a simple one-step radical polymerization (we termed these new material *Fluoropor*).<sup>[28]</sup> *Fluoropor* is formed via a light-induced polymerization of a PFPE-methacrylate in a nonsolvent (cyclohexanol) and an emulsifying agent (fluorinated alcohol). Due to the inherent nano-/microstructure throughout the whole bulk material the superhydrophobic properties are insensitive to abrasion. This is a major advantage over state-of-the-art superhydrophobic coatings such as deposited nanoparticles,<sup>[66–68]</sup> etched,<sup>[69,70]</sup> anodized,<sup>[71]</sup> or imprinted surfaces<sup>[72]</sup> or surfaces made by phase-separation effects<sup>[73,74]</sup> which are often fragile single layers and very sensitive to abrasion. Since the pore size of *Fluoropor* foam is smaller than the wavelength of visible light the material is optically transparent (see Figure 4a) making these materials applicable for real-world applications like window coatings, etc. Due to the possibility to cure *Fluoropor* via photopolymerization these materials are interesting candidates for 3D printing of chemically resistant coatings and components. Here, we demonstrate for the first time that *Fluoropor* can be printed using benchtop stereolithography printers and thus is accessible to 3D printing. The combination of printed superhydrophobic *Fluoropor* structures with a hydrophilic surface such as glass allows fabricating patterned surfaces which have gained significant interest in chemical synthesis of rare chemicals in droplets or open surface microfluidic reactors (see Figure 4b).<sup>[75,76]</sup> Since the polymerized *Fluoropor* samples possess a nonstructured top layer due to the polymerization process, superhydrophobic patterns can be fabricated by simply peeling off the last printed structured top layer. Future work will concentrate on superoleophobic/superoleophilic patterns enabling highly parallelized screening platforms for chemical synthesis.

## 6. Conclusion

We have provided an overview of current trends in the material development of high-performance materials which fulfill the requirements of chemical synthesis. We reviewed current work

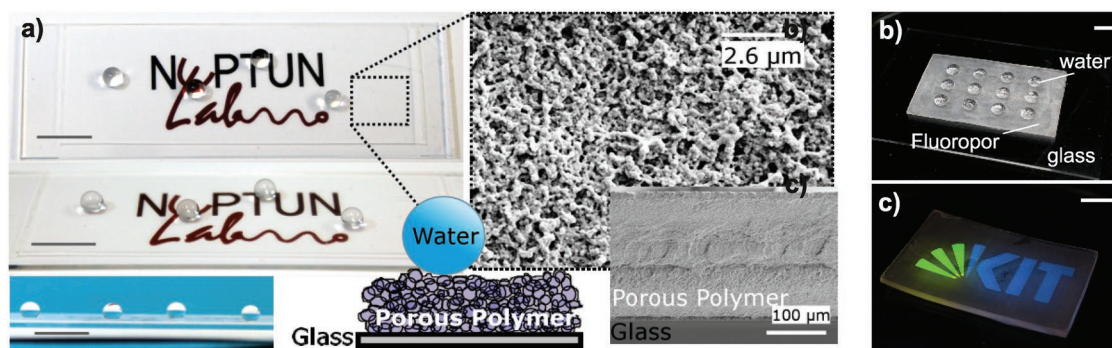


**Figure 4.** Porous and highly fluorinated polymers (termed *Fluoropor*) for chemical synthesis. a) Thin layers of *Fluoropor* (here: 105  $\mu\text{m}$ ) are highly optically transparent and show superhydrophobic properties (scale bars: 1 cm). Scanning electron microscope image displaying the micro/nanoporosity of polymerized *Fluoropor*. Reproduced with permission.<sup>[28]</sup> Copyright 2017, Springer. b) Patterned *Fluoropor* for droplet synthesis applications printed using stereolithography on a glass substrate. Pattern has been filled with water (scale bar: 10 mm). c) 3D-printed *Fluoropor* patterned by removing the top layer. Pattern has been filled with fluorescent dyes (scale bar: 10 mm).

in the field of 3D printing of chemically resistant transparent glasses, ceramics, and fluoropolymers. The advent of 3D printing offers significant potential for on-chip synthesis with the potential of reactant and solvent reduction therefore making the processes more economically and environmentally attractive. Miniaturization also significantly increases experimental throughput due to the inherent reduction in volume, increased thermodynamic control, shorter diffusion distances, and thereby faster reactions. However, most prominent is the potential for massive parallelization which will be key for the exploration and assessment of the chemical reaction space (pressure, temperature, stoichiometry, catalysts, etc.), candidate drug screening as well as optimization of synthesis conditions. To fully leverage these advantages, the design of tailored 3D printing materials will be key.

## 7. Experimental Section

**Materials:** Fluorolink MD700 was purchased from Acota (UK). 1H,1H,2H,2H-Perfluorooctanol was purchased from Apollo Scientific (UK). Diphenyl(2,4,6-trimethylbenzoyl) phosphine oxide (TPO) was purchased from Sigma Aldrich (Germany). Cyclohexanol and 2-propanol were purchased from Merck (Germany). Tinuvin 384-2 (T384-2) was kindly provided by BASF (Germany).

**Synthesis and 3D Printing of Fluoropor.** 50 wt% of Fluorolink MD700 was mixed with 20 wt% cyclohexanol and 30 wt% 1H,1H,2H,2H-perfluorooctanol. The mixture was blended with 0.6 wt% of the absorber T384-2 and 0.4 wt% of the photoinitiator TPO. *Fluoropor* was printed with a slice thickness of 50  $\mu\text{m}$  using the stereolithography printer Asiga Pico 2 purchased from Asiga (Australia). Printed parts were developed in 2-propanol for 2 d and left to dry for 1 d. The top layer of the 3D-printed parts was peeled off to create the superhydrophobic surface.

## Acknowledgements

This work was partly funded by the German Federal Ministry of Education and Research (BMBF), “Fluoropor,” funding code: 03X5527.

## Conflict of Interest

The authors declare no conflict of interest.

## Keywords

3D printing, additive manufacturing, fluoropolymers, fluoropor, transparent glass

Received: September 14, 2018  
Revised: November 21, 2018  
Published online: February 18, 2019

- [1] G. M. Whitesides, *Nature* **2006**, 442, 368.
- [2] A. Manz, J. C. Fettinger, E. Verpoorte, H. Lüdi, H. Widmer, D. Harrison, *TrAC, Trends Anal. Chem.* **1991**, 10, 144.
- [3] D. J. Harrison, A. Manz, Z. Fan, H. Luedi, H. M. Widmer, *Anal. Chem.* **1992**, 64, 1926.
- [4] D. Hülsenberg, A. Harnisch, A. Bismarck, *Microstructuring of Glasses*, Vol. 87, Springer, Berlin **2005**.
- [5] A. De Mello, *Lab Chip* **2002**, 2, 31N.
- [6] D. C. Duffy, J. C. McDonald, O. J. Schueller, G. M. Whitesides, *Anal. Chem.* **1998**, 70, 4974.
- [7] A. Waldbaur, H. Rapp, K. Lange, B. E. Rapp, *Anal. Methods* **2011**, 3, 2681.
- [8] N. Bhattacharjee, A. Urrios, S. Kang, A. Folch, *Lab Chip* **2016**, 16, 1720.
- [9] S. Waheed, J. M. Cabot, N. P. Macdonald, T. Lewis, R. M. Guijt, B. Paull, M. C. Breadmore, *Lab Chip* **2016**, 16, 1993.
- [10] W. Su, B. S. Cook, Y. Fang, M. M. Tentzeris, *Sci. Rep.* **2016**, 6, 35111.
- [11] C. M. B. Ho, S. H. Ng, K. H. H. Li, Y.-J. Yoon, *Lab Chip* **2015**, 15, 3627.
- [12] H. Gong, B. P. Bickham, A. T. Woolley, G. P. Nordin, *Lab Chip* **2017**, 17, 2899.
- [13] K. S. Elvira, X. C. i Solvas, R. C. Wootton, *Nat. Chem.* **2013**, 5, 905.
- [14] W. Ehrfeld, V. Hessel, V. Haverkamp, *Ullmann's Encyclopedia of Industrial Chemistry*, Wiley-VCH Verlag, Weinheim, Germany **2000**.
- [15] K. F. Jensen, B. J. Reizman, S. G. Newman, *Lab Chip* **2014**, 14, 3206.
- [16] K. F. Jensen, *Chem. Eng. Sci.* **2001**, 56, 293.
- [17] A. Adamo, R. L. Beingsner, M. Behnam, J. Chen, T. F. Jamison, K. F. Jensen, J.-C. M. Monbaliu, A. S. Myerson, E. M. Revalor, D. R. Snead, *Science* **2016**, 352, 61.
- [18] S. Sevim, A. Sorrenti, C. Franco, S. Furukawa, S. Pané, J. Puigmartí-Luis, *Chem. Soc. Rev.* **2018**, 47, 3788.
- [19] H. Kim, K.-I. Min, K. Inoue, D. J. Im, D.-P. Kim, J.-I. Yoshida, *Science* **2016**, 352, 691.
- [20] M. B. Plutschack, B. U. Pieber, K. Gilmore, P. H. Seeberger, *Chem. Rev.* **2017**, 117, 11796.
- [21] C. Parra-Cabrera, C. Achille, S. Kuhn, R. Ameloot, *Chem. Soc. Rev.* **2018**, 47, 209.

- [22] A. J. Capel, S. Edmondson, S. D. Christie, R. D. Goodridge, R. J. Bibb, M. Thurstans, *Lab Chip* **2013**, *13*, 4583.
- [23] S. Rossi, A. Puglisi, M. Benaglia, *ChemCatChem* **2018**, *10*, 1512.
- [24] P. J. Kitson, R. J. Marshall, D. Long, R. S. Forgan, L. Cronin, *Angew. Chem., Int. Ed.* **2014**, *53*, 12723.
- [25] A. I. Shallan, P. Smejkal, M. Corban, R. M. Guijt, M. C. Breadmore, *Anal. Chem.* **2014**, *86*, 3124.
- [26] M. Hegde, V. Meenakshisundaram, N. Chartrain, S. Sekhar, D. Tafti, C. B. Williams, T. E. Long, *Adv. Mater.* **2017**, *29*, 1701240.
- [27] Y. Zhang, M. Yin, O. Xia, A. P. Zhang, H.-Y. Tam, *Micro Electro Mech. Syst. (MEMS)* **2018**.
- [28] D. Helmer, N. Keller, F. Kotz, F. Stolz, C. Greiner, T. M. Nargang, K. Sachsenheimer, B. E. Rapp, *Sci. Rep.* **2017**, *7*, 15078.
- [29] a) M. Fateri, A. Gebhardt, *Int. J. Appl. Ceram. Technol.* **2015**, *12*, 53; b) F. Klocke, A. McClung, C. Ader, presented at *Solid Freeform Fabrication Symp. Proc.*, Austin, TX, August **2004**.
- [30] D. Bourell, B. Stucker, G. Marchelli, R. Prabhakar, D. Storti, M. Ganter, *Rapid Prototyping J.* **2011**, *17*, 187.
- [31] J. Klein, M. Stern, G. Franchin, M. Kayser, C. Inamura, S. Dave, J. C. Weaver, P. Houk, P. Colombo, M. Yang, N. Oxman, *3D Print. Addit. Manuf.* **2015**, *2*, 92.
- [32] J. Luo, H. Pan, E. C. Kinzel, *J. Manuf. Sci. Eng.* **2014**, *136*, 061024.
- [33] F. Kotz, K. Arnold, W. Bauer, D. Schild, N. Keller, K. Sachsenheimer, T. M. Nargang, C. Richter, D. Helmer, B. E. Rapp, *Nature* **2017**, *544*, 337.
- [34] F. Kotz, K. Plewa, W. Bauer, N. Schneider, N. Keller, T. Nargang, D. Helmer, K. Sachsenheimer, M. Schäfer, M. Worgull, C. Greiner, C. Richter, B. E. Rapp, *Adv. Mater.* **2016**, *28*, 4646.
- [35] F. Kotz, N. Schneider, A. Striegel, A. Wolfschläger, N. Keller, M. Worgull, W. Bauer, D. Schild, M. Milich, C. Greiner, D. Helmer, B. E. Rapp, *Adv. Mater.* **2018**, *30*, 1707100.
- [36] D. T. Nguyen, C. Meyers, T. D. Yee, N. A. Dudukovic, J. F. Destino, C. Zhu, E. B. Duoss, T. F. Baumann, T. Suratwala, J. E. Smay, R. Dylla-Spears, *Adv. Mater.* **2017**, *29*, 1701181.
- [37] I. Cooperstein, E. Shukrun, O. Press, A. Kamyshny, S. Magdassi, *ACS Appl. Mater. Interfaces* **2018**, *10*, 18879.
- [38] J. F. Destino, N. A. Dudukovic, M. A. Johnson, D. T. Nguyen, T. D. Yee, G. C. Egan, A. M. Sawvel, W. A. Steele, T. F. Baumann, E. B. Duoss, T. Suratwala, R. Dylla-Spears, *Adv. Mater. Technol.* **2018**, *3*, 1700323.
- [39] N. A. Dudukovic, L. L. Wong, D. T. Nguyen, J. F. Destino, T. D. Yee, F. J. Ryerson, T. Suratwala, E. B. Duoss, R. Dylla-Spears, *ACS Appl. Nano Mater.* **2018**.
- [40] K. Kajihara, *J. Asian Ceram. Soc.* **2013**, *1*, 121.
- [41] J. Zarzycki, M. Prassas, J. Phalippou, *J. Mater. Sci.* **1982**, *17*, 3371.
- [42] T. Wirth, *Microreactors in Organic Chemistry and Catalysis*, Wiley, New York **2013**.
- [43] N. Travitzky, A. Bonet, B. Dermeik, T. Fey, I. Filbert-Demut, L. Schlier, T. Schlordt, P. Greil, *Adv. Eng. Mater.* **2014**, *16*, 729.
- [44] A. Bertsch, S. Jiguet, P. Renaud, *J. Micromech. Microeng.* **2004**, *14*, 197.
- [45] M. Schwentenwein, J. Homa, *Int. J. Appl. Ceram. Technol.* **2014**.
- [46] P. Colombo, G. Mera, R. Riedel, G. D. Soraru, *J. Am. Ceram. Soc.* **2010**, *93*, 1805.
- [47] Z. C. Eckel, C. Zhou, J. H. Martin, A. J. Jacobsen, W. B. Carter, T. A. Schaedler, *Science* **2016**, *351*, 58.
- [48] E. Zanchetta, M. Cattaldo, G. Franchin, M. Schwentenwein, J. Homa, G. Brusatin, P. Colombo, *Adv. Mater.* **2016**, *28*, 370.
- [49] T. A. Pham, D. P. Kim, T. W. Lim, S. H. Park, D. Y. Yang, K. S. Lee, *Adv. Funct. Mater.* **2006**, *16*, 1235.
- [50] A. Urrios, C. Parra-Cabrera, N. Bhattacharjee, A. M. Gonzalez-Suarez, L. G. Rigat-Brugarolas, U. Nallapatti, J. Samitier, C. A. DeForest, F. Posas, J. L. Garcia-Cordero, *Lab Chip* **2016**, *16*, 2287.
- [51] X. Zhou, C. J. Liu, *Adv. Funct. Mater.* **2017**, *27*, 1701134.
- [52] C. R. Tubío, J. Azuaje, L. Escalante, A. Coelho, F. Guitián, E. Sotelo, A. Gil, *J. Catal.* **2016**, *334*, 110.
- [53] S. Couck, J. Lefevere, S. Mullens, L. Protasova, V. Meynen, G. Desmet, G. V. Baron, J. F. Denayer, *Chem. Eng. J.* **2017**, *308*, 719.
- [54] N. Jarvis, W. Zisman, DTIC Document, **1965**.
- [55] H. Teng, *Appl. Sci.* **2012**, *2*, 496.
- [56] 3M Cooperation, [https://www.3m.com/3M/en\\_US/design-and-specialty-materials-us/3d-printing/](https://www.3m.com/3M/en_US/design-and-specialty-materials-us/3d-printing/) (accessed: November 2018).
- [57] Z. Hu, J. A. Finlay, L. Chen, D. E. Betts, M. A. Hillmyer, M. E. Callow, J. A. Callow, J. M. DeSimone, *Macromolecules* **2009**, *42*, 6999.
- [58] Y. Huang, P. Castrataro, C.-C. Lee, S. R. Quake, *Lab Chip* **2007**, *7*, 24.
- [59] J. P. Rolland, R. M. Van Dam, D. A. Schorzman, S. R. Quake, J. M. DeSimone, *J. Am. Chem. Soc.* **2004**, *126*, 2322.
- [60] A. Priola, R. Bongiovanni, G. Malucelli, A. Pollicino, C. Tonelli, G. Simeone, *Macromol. Chem. Phys.* **1997**, *198*, 1893.
- [61] A. Vitale, M. Quaglio, S. L. Marasso, A. Chiodoni, M. Cocuzza, R. Bongiovanni, *Langmuir* **2013**, *29*, 15711.
- [62] C. Hannig, M. Dirschka, K. Länge, S. Neumaier, B. E. Rapp, *Proc. Eng.* **2010**, *5*, 866.
- [63] G. Maltezos, E. Garcia, G. Hanrahan, F. A. Gomez, S. Vyawahare, R. M. van Dam, Y. Chen, A. Scherer, *Lab Chip* **2007**, *7*, 1209.
- [64] F. Kotz, P. Risch, D. Helmer, B. E. Rapp, *Micromachines* **2018**, *9*, 115.
- [65] C. De Marco, A. Gaidukeviciute, R. Kiyam, S. M. Eaton, M. Levi, R. Osellame, B. N. Chichkov, S. Turri, *Langmuir* **2013**, *29*, 426.
- [66] X. Deng, L. Mammen, H.-J. Butt, D. Vollmer, *Science* **2012**, *335*, 67.
- [67] Y. Gao, I. Gereige, A. El Labban, D. Cha, T. T. Isimjan, P. M. Beaujuge, *ACS Appl. Mater. Interfaces* **2014**, *6*, 2219.
- [68] X. Zhang, H. Kono, Z. Liu, S. Nishimoto, D. A. Tryk, T. Murakami, H. Sakai, M. Abe, A. Fujishima, *Chem. Commun.* **2007**, 4949.
- [69] J. Fresnais, J. Chapel, F. Poncin-Epaillard, *Surf. Coat. Technol.* **2006**, *200*, 5296.
- [70] J.-H. Kong, T.-H. Kim, J. H. Kim, J.-K. Park, D.-W. Lee, S.-H. Kim, J.-M. Kim, *Nanoscale* **2014**, *6*, 1453.
- [71] M. Kemell, E. Färm, M. Leskelä, M. Ritala, *Phys. Status Solidi A* **2006**, *203*, 1453.
- [72] S. Liu, M. Sakai, B. Liu, C. Terashima, K. Nakata, A. Fujishima, *RSC Adv.* **2013**, *3*, 22825.
- [73] H. S. Hwang, N. H. Kim, S. G. Lee, D. Y. Lee, K. Cho, I. Park, *ACS Appl. Mater. Interfaces* **2011**, *3*, 2179.
- [74] F. Ouhib, A. Dirani, A. Aqil, K. Glinel, B. Nysten, A. M. Jonas, C. Jérôme, C. Detrembleur, *Polym. Chem.* **2016**, *7*, 3998.
- [75] E. Ueda, P. A. Levkin, *Adv. Mater.* **2013**, *25*, 1234.
- [76] Y. Han, P. Levkin, I. Abarientos, H. Liu, F. Svec, J. M. Fréchet, *Anal. Chem.* **2010**, *82*, 2520.
- [77] a) H. Zhu, M. Holl, T. Ray, S. Bhushan, D. R. Meldrum, *J. Micromech. Microeng.* **2009**, *19*, 065013; b) J. M. Nagarah, D. A. Wagenaar, *J. Micromech. Microeng.* **2012**, *22*, 035011.